Soft Matter

PAPER

View Article Online
View Journal | View Issue

Cite this: *Soft Matter*, 2026, **22**, 1402

Rheological matchup of real and plant-based mayo: gel strength, strain overshoot, and yielding, plus the extended Cox–Merz rule

Nadia N. Nikolova, [a] Stefan K. Baier[bc] and Vivek Sharma *[a]

Mayonnaise is a dense oil-in-water emulsion with over 65% oil, vinegar (or lime juice), and egg as an emulsifier or stabilizer. Conventional mayonnaise, an animal-based (AB) formulation, has flow behavior suitable for dispensing, spooning, spreading, consuming, and use as a salad dressing, dip, and base for sauces. Emulating its texture, flavor, stability, rheology, processability, and sensory attributes is challenging with egg-free recipes that often include plant-based (PB) proteins and hydrocolloids, such as xanthan gum, guar gum, and starch in the aqueous phase. Here, we contrast the rheological responses of commercially available AB and PB mayos under oscillatory strain to assess their linear and nonlinear viscoelastic properties and to assess why the addition of hydrocolloids provides an egg-free alternative with suitable shelf-life and processability. Also, responses assess texture and the first-bite impression and help contrast the mouthfeel that encompasses holistic and dynamic sensations throughout consumption. All mayos display gel-like responses in oscillatory shear at low strain and liquid-like responses beyond the yield stress. All AB mayos show a strain overshoot in the plots of loss modulus against strain, which is absent in the response of vegan mayos that use polysaccharides as hydrocolloids. We contrast the apparent yield stress values from the shear flow curve, the onset of strain softening in the elastic modulus beyond a critical strain, and dripping experiments. Hydrocolloids and proteins with dissimilar interfacial and bulk properties contribute to the contrasting moduli, yielding, and strain overshoot response of real and vegan mayo.

Received 28th July 2025,
Accepted 14th January 2026

DOI: 10.1039/d5sm00775e

rsc.li/soft-matter-journal

Introduction

Animal-based (AB) or real mayonnaises are jammed, dense emulsions with relatively high oil volume fractions ($\phi > 65\%$), leading to drops with polygonal shapes separated by thin films that form a network reminiscent of foam architecture.[1–6] Such a microstructure results in a gel-like response to oscillatory shear strain, and a flow curve with an apparent yield stress, σ_y, and exhibits a significant decrease in viscosity (increase in fluidity) as the applied stress ($\sigma > \sigma_y$) is progressively raised above the yield value.[1,4–11] As the FDA in the USA requires mayonnaise to include yolk-containing ingredients, the egg-free alternative to "real" mayonnaise[12,13] is referred to as plant-based (PB) or vegan mayo, vegenaise, or a dressing and spread. In 2023, the global plant-based food market was valued at ~$27 billion and is expected to double by 2030. Manufacturers are increasingly designing plant-based alternatives to animal-based foods, driven by consumer demand and concerns about sustainability, animal welfare, climate change, health (including fat, nutrients, and microbes), religious or cultural preferences, evolving supply chains, and food allergies.[6,14–17] However, designing PB alternatives is challenging because it requires characterizing and emulating the physicochemical properties, taste, texture, mouthfeel, shelf-life, processability, and overall consumer satisfaction of the corresponding animal products.[5,7,18–20] Considerations include dispensing, spreading, dipping, handling, chewing, and swallowing behavior, as well as aftertaste, digestibility, and health benefits.[5,7,18–20] Several of the consumer-based sensory preferences described in terms such as mouthfeel (*e.g.* creaminess or smoothness), texture (*e.g.* gel strength or firmness), flowability (*e.g.* thickness, cohesiveness, or gloopiness), and manufacturer's criteria for ingredients and processability can be translated into rheological quests for deciphering and describing yielding, consistency, gel strength, and flow behavior. The grand challenge is to establish which rheological parameters and experimental protocols best capture the requirements and preferences of manufacturers and consumers, while enabling fundamental insights into the molecular engineering of food and first-principles description of its flow behavior. In this contribution, we characterize the linear and nonlinear

[a] *Department of Chemical Engineering, University of Illinois Chicago, Chicago, IL 60607, USA. E-mail: viveks@uic.edu*
[b] *Motif Foodworks, Boston, MA, USA*
[c] *School of Chemical Engineering, The University of Queensland, Brisbane, QLD 4072, Australia*

viscoelastic responses of AB and PB mayos *via* oscillatory shear, comparing the yield stress, yielding behavior, and viscosity with values measured in the response to progressively varying strain rates or stresses.

Egg influences the emulsification, flavor, emulsion stability, and rheology of real mayonnaise. Egg yolk contains an abundance of amphipathic lipids, proteins, and lipoprotein complexes (livetin, phosvitin, lipovitellin, and lipovitellenin), whereas egg white is rich in proteins (ovalbumin, ovotransferrin, ovomucoid, ovomucin, and lysozyme).[21] The plant-based (PB) alternatives incorporate ingredients like aquafaba or soy milk, which contain plant proteins that are expected to serve as emulsifiers, and provide nutrition, flavor, and rheological response.[1,2,22–24] Plant proteins tend to be mainly globular, with four sub-classifications based on solubility criteria: albumins (in water), globulins (in dilute salt solutions), prolamins (in aqueous ethanol solutions), and glutelins (in dilute acid/alkaline solutions, but insoluble in water).[24] As egg proteins, which are also globular, tend to be more water-soluble and better emulsifiers, the egg-free recipes sometimes supplement PB proteins with lipids to facilitate emulsification and enhance emulsion stability.[25] Often, PB emulsions incorporate small molecules to enhance the flavor profile and hydrocolloids, such as starches or polysaccharides, to influence interfacial and suspending liquid properties, enhancing emulsion stability and tuning rheology and processability.[26–30] A rational formulation design requires a fundamental understanding of how ingredients influence the mayo microstructure, dynamics of dispersed drops and macromolecules, flows within the suspending fluid, and the deformation and flow of interfaces.[6,7,31–36] Our review of the current state-of-the-art in modeling drop deformations and emulsions rheology[37] lists the many unresolved challenges that arise in understanding the influence of non-Newtonian suspending fluids and interfaces on emulsion rheology.[6,31–37] Despite considerable literature on the shear rheology response of animal-based and low-fat mayos,[3,16,38–44] the rheology of vegan mayos remains relatively uncharted.[4,17,22,45,46] Although we ultimately aim to elucidate and design ingredient-dependent rheology for emulsions, here we focus on characterizing the contrasting rheology of commercially available AB and PB mayos.

The oscillatory shear rheometry provides two primary measures of moduli: storage or elastic modulus, G', and loss or viscous modulus, G'', obtained by varying the strain amplitude, γ, at a constant oscillation frequency, ω, or *vice versa*, as summarized in Fig. 1.[7,47] The G' variation captures the elastic or the solid-like response, as the measured stress, σ_{12} is in phase ($\delta = 0$) with the applied strain, γ. The G'' variation captures the dissipative, liquid-like response, with the σ_{12} as out of phase ($\delta = \pi/2$) with γ. The moduli G' and G'' appear nearly constant for sour cream at low strain as shown in Fig. 1a, which corresponds to the linear viscoelastic (LVE) regime.[48] Small amplitude oscillatory shear (SAOS) measurements utilize frequency sweeps at small strain to capture the characteristic LVE responses of complex fluids, with frequency-dependent moduli displaying the influence of elasticity, dynamics, and dissipation by the weakly perturbed microstructure of complex fluids.[7] Nonlinear VE response measured in so-called LAOS measurements (and the MAOS regime is in a transition regime or asymptotically nonlinear regime), and in a more generalized framework, $G'(\omega)$

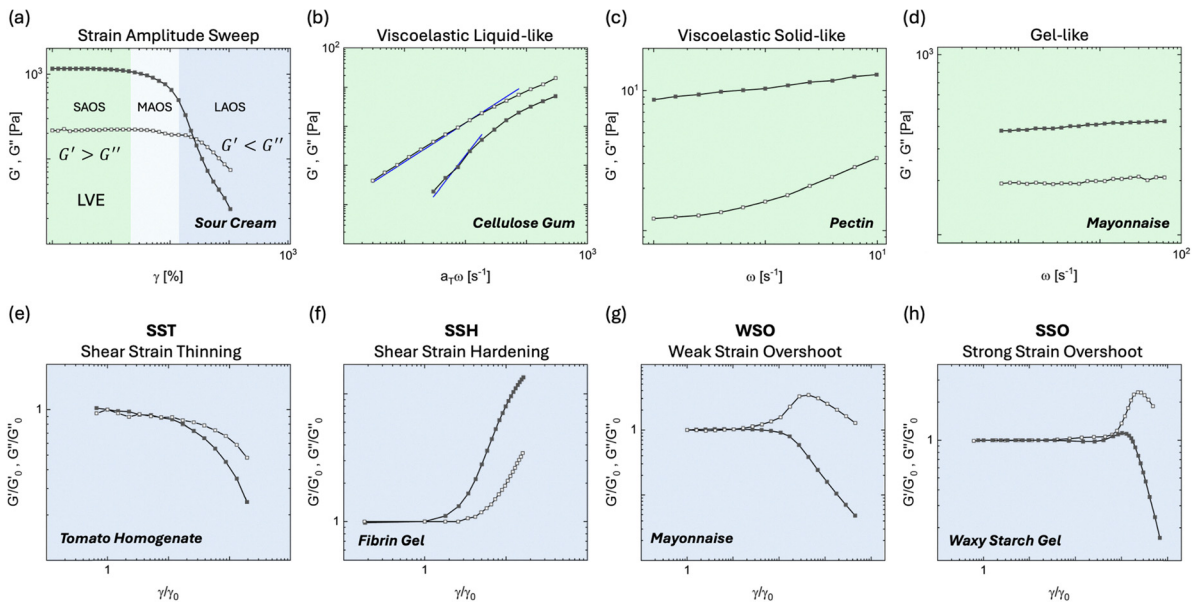

Fig. 1 Illustrations of rheological behavior displayed by food as soft matter (or edible soft matter) in oscillatory shear rheometry. (a) Strain sweep at fixed frequency for Daisy-brand sour cream,[48] illustrating three regimes: small, medium, and large amplitude oscillatory shear (SAOS, MAOS, and LAOS). Frequency sweep obtained using SAOS with three typical characteristics: (b) viscoelastic liquid-like response of 1 wt% of cellulose gum in an aqueous solution;[52] (c) viscoelastic solid-like response of Ca^{2+} F-pectin gel;[53] (d) gel-like response of real mayonnaise with 80% oil fraction.[3] Four key types of nonlinear responses revealed *via* strain sweep (in LAOS experiments): (e) shear strain thinning (SST) for high-pressure treated tomato homogenate.[54] (f) Shear strain hardening (SSH) for fibrin gel.[56,57] (g) Weak strain overshoot (WSO) for a 20 wt% oil AB mayo thickened with 6 wt% waxy corn starch.[41] (h) Strong strain overshoot (SSO) for 10 wt% waxy rice cultivar starch gel.[58]

and $G''(\omega)$ measured using SAOS represent only the first harmonic of a richer response function.[49–51] Using examples from food systems, Fig. 1b–d illustrate the $G'(\omega)$ and $G''(\omega)$ data obtained for a representative VE liquid (cellulose gum solution),[52] VE solid (pectin),[53] and mayonnaise as a gel-like material.[3] Fig. 1e–h show that amplitude sweep at a constant ω reveals the four key behavior types for the moduli $G'(\gamma)$ and $G''(\gamma)$ illustrated by for tomato homogenate,[54,55] fibrin gel,[56,57] low-fat mayonnaise,[41] and a starch gel:[58] shear strain thinning (SST), shear strain hardening (SSH), weak strain overshoot (WSO), and strong strain overshoot (SSO) (also referred to as type I, II, III, and IV, respectively).[41,49–61] Strain thinning is alternatively referred to as strain softening and strain hardening as strain stiffening.

Real mayonnaise has nearly frequency-independent moduli in the LVE regime, as shown in Fig. 1d.[3] The perceived "gel" texture is captured below a critical strain, as shown in Fig. 1g. In the strain sweep, the loss modulus $G''(\gamma)$ of AB mayonnaise exhibits an overshoot, displaying the WSO response. A structural breakdown of the gel network occurs above a critical strain, and the elastic modulus $G'(\gamma)$ for this jammed-dense emulsion displays a yield point. Thus, mayonnaise, like many food products, exhibits yield stress, σ_y which also contributes to the product's texture and mouthfeel during consumption and its flow behavior during dispensing, dipping, or spreading.[9,62–64] A wide range of yield stress values, from $\sigma_y \sim 20$ Pa to $\sigma_y \sim 200$ Pa, has been reported for commercially available and homemade mayonnaise.[3,16,38–43] Unfortunately, as there is no single agreed-upon method for estimating or measuring yield stress, the reported values vary considerably depending on the type of flow experiment being performed.[8,9,11,63–66] We previously characterized the apparent σ_y and shear thinning behavior of AB and PB mayos using torsional rheometry[4] and determined the apparent extensional yield stress, σ_{ye}, and dispensing behavior using dripping experiments.[4] Though all mayos displayed yielding, shear thinning, and two regimes in pinching (intermediate power law and terminal linear variation of radius with time), most real mayos showed higher σ_y and σ_{ye} values compared with vegan mayos.[4] Even for real and vegan mayos that displayed comparable rate-dependent viscosity, implying that manufacturers can employ similar processing equipment and parameters, we found striking differences in the dispensing behavior and the extensional rheology response.[4] However, our previous publication and the state-of-the-art published literature lack a comparative characterization of the oscillatory shear response of AB and PB mayos, even though in industrial practice, the oscillatory shear responses are often characterized, mapped and correlated to consumer-perceived desirables and distinctions in texture, consistency, viscosity, dispensing, spreadability, first bite impression, mouthfeel, and cohesion.[50,67–73]

The magnitude of complex viscosity, $|\eta^*(\omega)|$ obtained as a function of fixed low or high strain and variable frequency, ω can be compared to the shear rate-dependent variation in viscosity, $\eta(\dot{\gamma})$. Complex fluids, such as entangled polymer solutions and melts, display a fortuitous agreement $\eta(\dot{\gamma}) = |\eta^*(\omega)|_{\omega=\dot{\gamma}}$, also known as the Cox–Merz rule, for $|\eta^*(\omega)|$ obtained using small-amplitude oscillatory shear (SAOS) measurements in the linear viscoelastic regime (LVE). For polymeric materials, the Cox–Merz rule (and time-temperature superposition) enables acquisition of flow curves over an extended shear rate range, even though elastic instabilities and instrument limitations plague such measurements in drag-driven or pressure-driven rheometers.[74–76] The empirical Cox–Merz rule appears to hold for some food materials containing dispersions of starches, polysaccharides, and pectin.[77–79] However, it does not typically apply to concentrated and dense food systems, including tomato pastes,[80] dispersions of waxy maize[81] and tapioca starch,[82] wheat flour dough,[83] yogurt, condensed milk and cream cheese,[84] mayonnaise,[84,85] and other spreads such as apple butter, mustard, and margarine.[85] In 1991, Doraiswamy *et al.*[75] introduced an empirical extension of the Cox–Merz rule for complex fluids with a yield stress, and incorporated elastic, viscous, and yielding phenomena *via* a limiting recoverable strain. The modified Cox–Merz rule,[75] also known as the Rutgers–Delaware rule (as suggested by Krieger[86]), *i.e.* $\eta(\dot{\gamma}) = |\eta^*(\gamma_0\omega)|_{\dot{\gamma}=\gamma_0\omega}$ superimposes $(\eta(\dot{\gamma}))$ and the nonlinear viscoelastic response $(|\eta^*|(\gamma_0\omega))$ computed at an effective shear rate, using as a shift factor the critical strain defined at the point of yielding. Doraiswamy *et al.*[75] argued that even though the response to large-amplitude oscillatory shear involves many harmonics, the first harmonics determine all the parameters in their model. Here, we contrast the linear and nonlinear viscoelastic regimes and examine the response of AB and PB mayos using the conventional and the extended Cox–Merz rules.

The paper presents a rheological matchup of commercially available real and vegan mayos, with the typical fat content exceeding 70% by volume. Oscillatory shear tests evaluate moduli, gel strength, yield stress, and post-yielding behavior as a function of strain and frequency. The magnitude of the complex viscosity is compared with the rate-dependent viscosity to assess the applicability of the conventional and the extended Cox–Merz rules. Thereafter, the yield stress values estimated from oscillatory shear are compared with those deduced from shear flow curves and dripping experiments. We anticipate that the experimental protocols and distinctions described here will aid in deciphering how replacing AB proteins with PB proteins and additives, such as starch and polysaccharides that can influence interfacial properties and suspending liquid (or matrix) rheology, affect the overall flow behavior and sensory perception of mayos and other multi-ingredient edible soft matter.

Materials and methods

Three animal-based (AB or real) and four plant-based (PB or vegan) commercially available mayo samples were chosen for the study. The samples include two popular real mayonnaise brands, Hellmann's (Unilever PLC) and Kraft (Kraft Heinz Company). We also carefully chose two brands for which vegan counterparts were available: Hellmann's and Sir Kensington's (Unilever PLC). These mayos were also featured in our previous examination of shear and extensional rheology,[4] which

Table 1 Emulsifiers and thickeners of seven chosen commercial real mayonnaises and vegan mayos, and their fat content per tablespoon (tbsp) [or weight % of fat]

Sample name	Fat (g) per tbsp (g) [wt%]	Ingredients influencing rheology and emulsion stability
Hellmann's real mayonnaise	11/14 [79%]	Whole eggs, egg yolk
Sir Kensington's classic mayonnaise	11/14 [79%]	Egg yolks
Kraft real mayonnaise	10/13 [77%]	Eggs, egg yolks
Hellmann's plant-based mayo	8/14 [57%]	Modified potato starch, corn starch
Sir Kensington's classic vegan mayo	10/13.5 [74%]	Chickpea, acacia gum, xanthan gum
Chosen Foods classic vegan mayo	10/14 [71%]	Chickpea, faba bean, sunflower lecithin, xanthan gum, acacia gum, guar gum, mustard flour
Follow Your Heart original vegenaise	9/14 [64%]	Soy protein, brown rice syrup, mustard flour

complements this investigation. Table 1 lists the primary emulsifier, and the thickener among the ingredients, identified from the packaging labels for each sample. This table does not list the oils and the ingredients found in all samples, like lemon juice, vinegar, water, salt, and other additives, such as preservatives. Among the AB mayonnaises, Sir Kensington's brand only utilizes yolks, whereas whole eggs appear on the ingredient lists for the other two. The commercial real mayos typically contain pasteurized eggs and the aggregation, interfacial activity and conformational state of proteins are distinct from fresh eggs. No additional hydrocolloids are added to the AB mayos, whereas PB or vegan mayos invariably contain hydrocolloids like starches and gums. Sir Kensington's and Chosen Foods PB mayo contain polysaccharide thickeners, including xanthan gum and acacia gum. However, Hellmann's vegan mayo contains a combination of starches without the addition of gums or plant-based proteins. All three other PB mayos use plant protein sources, including chickpea or aquafaba (canned chickpea brine), soy, and faba bean. Chosen Foods mayo also incorporates sunflower lecithin, which acts as an emulsifier. Follow Your Heart mayo only uses a combination of soy, rice, and mustard byproducts to achieve the desired texture, bypassing polysaccharide gums.

Torsional rheometry measurements were performed on an Anton Paar MCR 302 rheometer at 25 °C. Roughened 25 mm parallel plates were created by applying a 600-grit adhesive-back sandpaper (McMaster-Carr Part #47185A51) to the smooth plates with a 1 mm sample testing gap. Amplitude sweep tests were performed within the low frequency range, at $\omega = 1$ rad s^{-1}, over a range of strain $\gamma = 0.01\%$ to $\gamma = 100\%$. The amplitude setting for the frequency sweep experiments was chosen to be within the linear viscoelastic (LVE) regime of each sample. The frequency sweep range was $\omega = 0.01$ rad s^{-1} to $\omega = 100$ rad s^{-1} to probe long and short time oscillations. Flow curves were obtained by ramping up from $\dot{\gamma} = 0.01$ s^{-1} to $\dot{\gamma} = 1000$ s^{-1}. To reduce the effects of deformation history from sample loading, a 10-minute wait time was implemented to allow time for restructuring and relaxation. The sample was replaced after each trial. Drop size distribution was obtained using a Bruker TD-NMR (time-domain) drop size analyzer.

Results

Strain sweep response and yielding *via* oscillatory shear

Amplitude strain sweeps are shown for real mayonnaise in the top row of Fig. 2(a)–(c) and for vegan mayos in the bottom row of Fig. 2(d)–(f). The critical strain, γ_c, shown using the dashed line in Fig. 2 at $\gamma = \gamma_c$, is identified as the strain amplitude corresponding to a drop in storage modulus to $0.9G_0' \approx G_c'$. The G' and G'' exhibit strain-independent values G_0' and G_0'', respectively, at low strain ($\gamma < \gamma_c$) for all real and vegan mayos. As moduli exhibit strain independence for $\gamma < \gamma_c$, the behavior indicates a linear viscoelastic (LVE) response. Here $G'(\gamma) > G''(\gamma)$, implying that the mayos appear solid-like under small deformations or stress. The real mayonnaise emulsions exhibit an elastic modulus at low strain or gel strength, $G_0' \approx 1000$ Pa, whereas the G_0' values for vegan mayo emulsions vary over a considerable range, from $G_0' \approx 150$ Pa to $G_0' \approx 2500$ Pa. Beyond the LVE regime, *i.e.*, for $\gamma > \gamma_c$, the samples exhibit a significant drop in the G' value or show yielding. The values of G' and G'' intersect at crossover strain, γ_x shown using the vertical dotted lines. Indeed, a transition from elastic-dominated to the viscous-dominant bulk response occurs above γ_x. As elastic modulus displays strain softening above γ_c, and the moduli shift from a solid-like response, with $G'(\gamma) > G''(\gamma)$ to a liquid-like response with $G'(\gamma) < G''(\gamma)$ response above γ_x, either strain can be referred to as a yield point. The corresponding plots for strain-dependent variation of tan δ is included as Fig. SF1 in the supplementary document. Fig. 2 shows that the vegan mayos yield at a lower strain, independent of the criteria used. A close comparison of the strain-dependent variation of storage modulus, G' and loss modulus, G'' for Hellmann's real and vegan mayos reveals a nearly matched magnitude and strain-dependent variation, reminiscent of close agreement displayed by variation of their viscosity with shear rate.[4] In contrast, Sir Kensington's real and vegan mayos display noticeable differences in the onset of yielding in the strain-dependent variation of $G'(\gamma)$ and the contrasting response of the loss modulus, $G''(\gamma)$. The paired comparison of strain variation of $G'(\gamma)$ and $G''(\gamma)$ of AB and PB mayos for these two brands are included in the two plots of Fig. SF2 in the supplementary document.

Fig. 2a–c show that the loss modulus, G'' for the real mayonnaise increases for $\gamma > \gamma_c$ ($\approx 10\%$) and then decreases with larger strain. Thus, the strain sweep reveals that all real mayonnaises or AB mayos exhibit weak strain overshoot (WSO), in agreement with previous studies (see Fig. 1 for example).[41] The extent of this strain-hardening, or strain overshoot, is weaker and less pronounced for Hellmann's and Follow Your Heart vegan mayos (see Fig. 2d and f). As these are the two PB mayos that contain hard granules from corn, potato, and/or

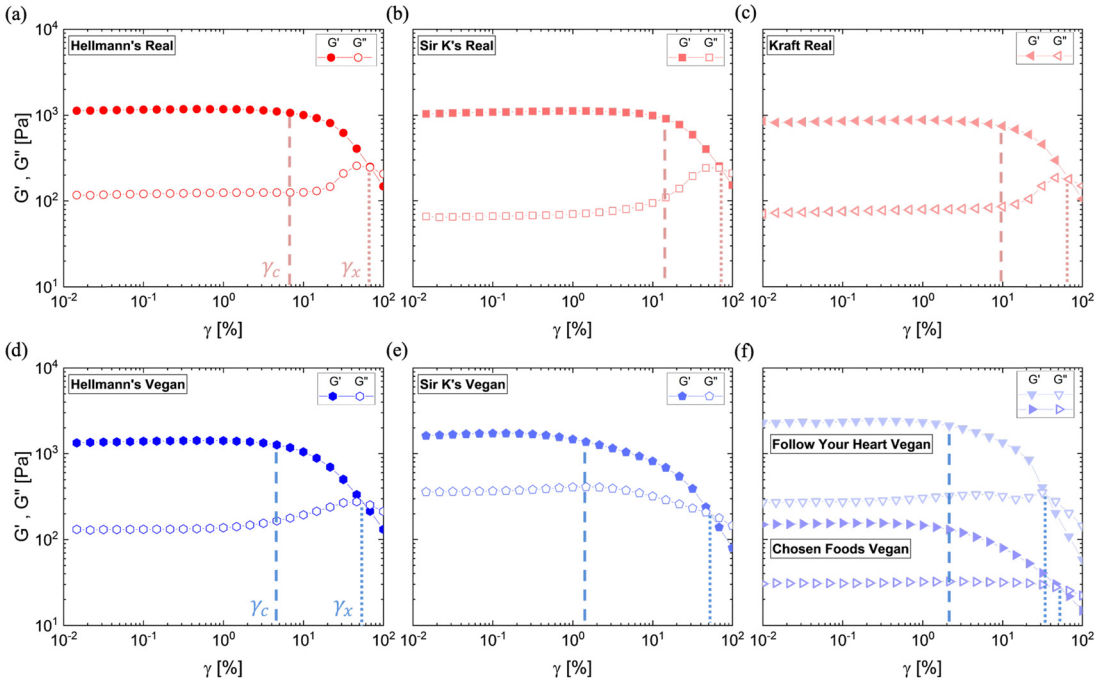

Fig. 2 Storage and loss moduli obtained using amplitude sweeps and critical strains for yielding of animal and plant-based mayo emulsions. Strain-dependent moduli - of (a) Hellmann's, (b) Sir Kensington's, (c) Kraft real mayonnaises, and (d) Hellmann's, (e) Sir Kensington's, (f) Follow Your Heart and Chosen Foods vegan mayos. Geometry used: roughened 25 mm parallel plates at 25 °C. Vertical dashed lines indicate the critical point, $0.9G_0'$, as a 10% reduction of storage modulus from the LVE region G_0'. Vertical dotted lines indicate the crossover point of G' and G''. Note the overlapping dashed lines in (f) for the two samples.

brown rice, the WSO arises, possibly due to droplet interface interactions that resist flow past other drops and granules at lower strains. In contrast, the oil droplets can deform and flow past other drops and the deformable granules at high strain. Alternatively, the strain-hardening bump could be interpreted as a contribution from the gel-like microstructure, which breaks down after a certain strain. This phenomenon has been observed in other studies of strain-dependent rheological response of foams and emulsions.[87,88] The two PB samples, Sir Kensington's and Chosen Foods (Fig. 2e and f), that contain polysaccharide additives such as acacia gum, xanthan gum, and guar gum display shear strain-thinning (SST) response (similar to the response of polysaccharide solutions for the relevant concentrations[60] and tomato homogenates[54,55]) as both moduli G' and G'' decrease with increasing strain after an initial strain-independent regime.

Frequency sweep response and gel strength *via* oscillatory shear

Moduli measurements *via* frequency sweeps included in Fig. 3 were performed at a relatively low strain, γ = 0.1% so at the chosen strain amplitude, the oscillatory shear response lies within the linear viscoelastic (LVE) regime, as determined from the strain amplitude sweeps. All mayos display a gel-like response, with $G'(\omega) > G''(\omega)$. Hellmann's and Kraft real mayonnaise storage and loss moduli in Fig. 3a and c show nearly frequency independence across the entire range, indicative of an elastic material or gel-like response. Sir Kensington's real mayonnaise, as well as Hellmann's and Follow Your Heart vegan mayos in Fig. 3b, d, and f show a slight increase in the loss modulus at higher frequencies. In Fig. 3e and f, Sir Kensington's and Chosen Foods vegan mayos, which contain gum additives, both G' and G'' increase slightly with increasing frequency, and the Chosen Foods exhibits a weaker elastic response than the other samples. All AB mayonnaises show comparable gel strength, or $G' \sim 1000$ Pa and loss modulus, $G'' \sim 100$ Pa. In contrast, PB mayos exhibit a considerable range of values for apparent gel strength (100 Pa $< G' <$ 2000 Pa) and loss modulus (25 Pa $< G'' <$ 300 Pa) Hellmann's real and vegan mayo display comparable loss modulus value, $G'' \sim 100$ Pa, but Sir Kensington's real mayo exhibits a lower value. Sir Kensington's vegan mayo exhibits a higher loss modulus and greater energy dissipation than other PB mayos, as shown in Fig. 3. Strain sweep measurement with a lack of overshoot in G'' and frequency sweep measurement with weak variation in G' set Sir Kensington's vegan mayo apart compared to its real counterpart and Hellmann's real and vegan mayos.

The changes in elastic and loss modulus as a function of strain amplitude and frequency shown in Fig. 2 and 3 provide insights into gel strength, yielding, microstructural changes, and contributions to the flow response. The continuous phase forms thin films between the deformable dispersed phase droplets in the jammed, dense emulsion, resulting in a foam-like polyhedral packing. As strain is applied, the drops deform in alignment with the flow, causing the bulk behavior to transition from elastic to viscous. Additionally, the magnitude

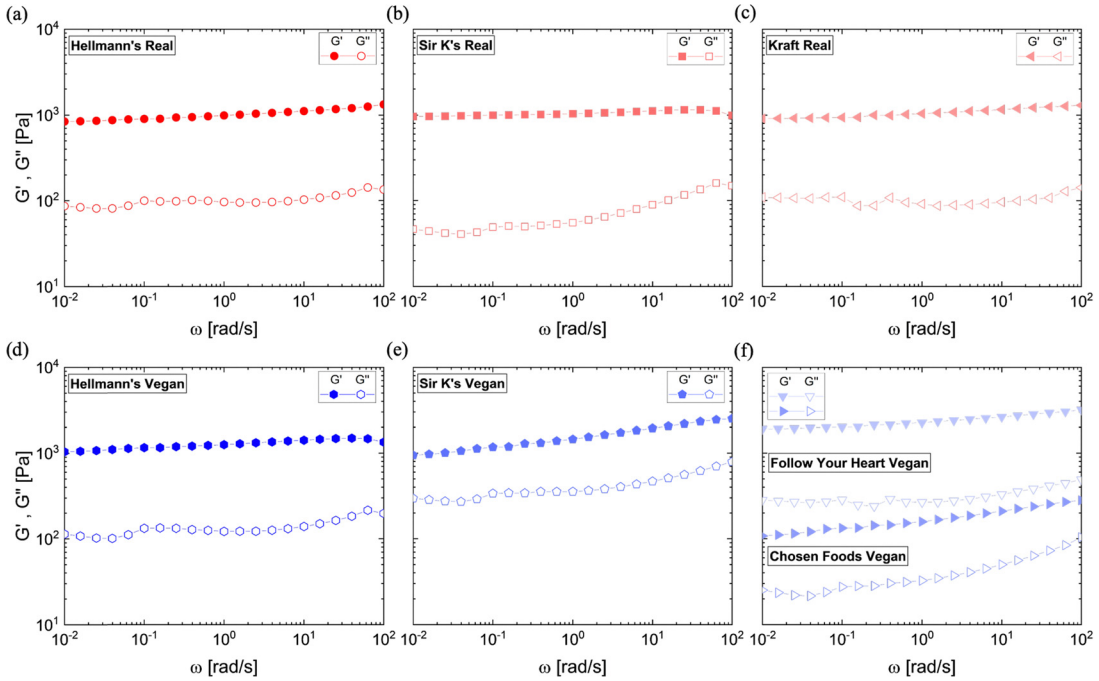

Fig. 3 Oscillatory frequency sweep rheology of animal and plant-based mayo emulsions. Storage and loss moduli in linear viscoelastic (LVE) regime characterized by frequency sweeps at low applied strain of (a) Hellmann's (b) Sir Kensington's (c) Kraft real mayonnaises and (d) Hellmann's (e) Sir Kensington's (f) Follow Your Heart and Chosen Foods vegan mayos. Geometry used: roughened 25 mm parallel plates at 25 °C.

and variation of G' and G'' can also indicate heuristic and sensory properties described as initial texture perception, firmness, and gel strength of a soft material like mayonnaise.[18,89] The gel strength of real mayonnaises in this study (G' = 1000 Pa) corresponds to previous measurements of commercial and model mayonnaise emulsions.[3,90,91] In contrast, the vegan mayos exhibit a broader range of the elastic moduli values (G' = 100 Pa to G' = 2000 Pa) implying it is more challenging to predict and control the apparent gel strength consistently compared to AB mayonnaise. Although the evaluation using moduli data from amplitude sweep measurements consistently shows all real mayos have higher apparent yield stress than vegan mayos, the moduli measured in response to oscillatory frequency sweep in the LVE regime shows mixed results, with some vegan mayos showing higher modulus values.

Drop sizes and composition of mayos

We obtained the drop-size distribution and fat composition for a representative subset of four samples: Hellmann's real and vegan mayos, Sir Kensington's real mayonnaise, and Follow Your Heart vegan mayo. Many previous studies show optical or confocal microscopy images of the AB mayonnaise drops as $\sim O$(1–10 μm), arguing that these are significantly smaller and more uniform in size than those formed in vegan mayos.[22,45,92–95] Unfortunately, optical microscopy measurements at high drop volume fractions are affected by high opacity, sampling errors, and perturbing structures during sample transfer between cover slips. Confocal microscopy additionally requires staining with fluorescent dyes or using fluorescent molecules or macromolecules.[2,22,41,96] Scattering, commonly used to determine drop sizes in dilute and semi-dilute emulsions, cannot be used for concentrated and jammed-dense emulsions without significant dilution (see protocols outlined for use with Malvern Mastersizer, Horiba's Partica or Extregis Accusizer).[22,94] Furthermore, methods relying on scattering cannot distinguish between drops and particulate matter such as proteins and starches. We therefore decided to obtain drop sizes using TD-NMR (time-domain nuclear magnetic resonance), a non-invasive technique that requires no dilution, is well-suited to dense and opaque emulsions, and can distinguish between drops and particles.[97–100]

Table 2 provides metrics to assess size variation and also includes the composition, expressed as percent moisture and fat. Hellmann's real, Sir Kensington's real, and Follow Your Heart vegan appear to have relatively high fat fractions, suggesting their rheology has a similar microstructural origin: a continuous phase in the form of a network of thin films between deformable dispersed-phase droplets, resulting in a foam-like polyhedral packing.[2] The elastoviscoplastic response, characterized by a yield stress, strain-dependent elastic and viscous moduli, and shear-thinning behavior, is therefore reporting the integrated response of the foam-like network and the drops to applied stress.[37,101–105] In Table 1, we list fat content per tablespoon (wt%) for all samples based on their labels, and the simplest estimates of volume fraction for the four mayos included in Table 2 are in reasonable agreement with the labels. Therefore, we can estimate that Kraft real and Sir Kensington's vegan mayos also have $\phi > 70\%$ and are jammed-dense emulsions. However, as the Hellmann's plant-based mayo has a relatively low fat fraction (54%), the elasticity and yielding response are not just due to the foam-like architecture but are deeply influenced by

Table 2 The fat composition and oil drop sizes in real and vegan mayos

	Diameter (μm)				Composition	
Sample description	D2.5 (2.5%)	D50 (50%)	D97.5 (97.5%)	δ*D* (stdev)	Moisture (%)	Fat (%)
Hellmann's real mayo	1.61	2.71	4.56	0.74	17	78
Hellmann's plant based mayo	1.96	3.05	4.74	0.70	41	54
Sir Kensington's classic mayo	1.02	1.78	3.14	0.53	14	82
Follow Your Heart-original vegan	1.64	3.51	7.52	1.47	23	72

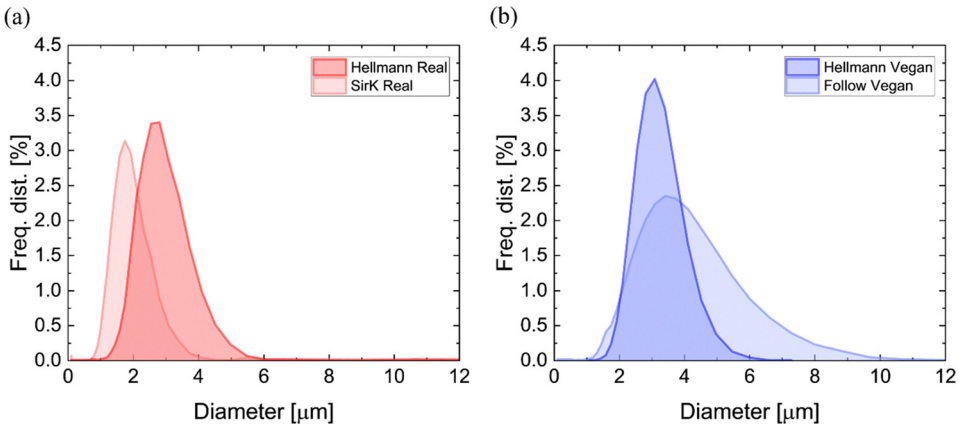

Fig. 4 Drop size distributions of animal and plant-based mayo emulsions determined *via* TD-NMR. Drop sizes of (a) Hellmann's and Sir Kensington's real mayonnaises and (b) Hellmann's and Follow Your Heart vegan mayos are of the order of a few microns. Real mayonnaise showed smaller drop diameters compared to the vegan mayos sampled.

the dynamics of the modified starch present at the interface and in the suspending liquid.

Table 2 lists the drop diameters D2.5, D50, and D97.5, below which, respectively, 2.5%, 50%, and 97.5% of the drops in the distribution fall. Here, D50 provides a measure of the median size, whereas D2.5 and D97.5 represent the fines and large drops at the tail ends of the distribution. Of the two Hellmann's mayos, the vegan mayo appears to have greater polydispersity and larger drop sizes. The average drop sizes for Follow Your Heart vegan mayo are larger than the other three, whereas Sir Kensington's real mayonnaise has the smallest drop sizes. Fig. 4 shows the corresponding drop size distribution obtained from the analysis of hindered diffusion in these NMR studies: Sir Kenginston's mayonnaise has the narrowest size distribution. Table 2 and Fig. 4 indicate that Follow Your Heart mayo has the widest size variation.

Viscoelasticity of mayo emulsions and the extended Cox–Merz rule

The flow curves showing viscosity as a function of shear rate are compared in Fig. 5 to the complex viscosities, $|\eta^*|(\gamma_0\omega)$, plotted as a function of effective shear rate, using chosen strain amplitude γ_0 and frequency values. Shear viscosity data for all mayos display shear thinning over this range of shear rates. Consistently, $|\eta^*|$ datasets also exhibit shear-thinning for the range of frequencies tested. However, the range of effective shear rates depends on γ_0, with values spanning the range from the LVE to the nonlinear regime. Fig. 5 shows that the Cox–Merz rule $(\eta(\dot{\gamma}) = |\eta^*(\omega)|_{\omega=\dot{\gamma}})$ that uses the LVE data (for γ_0 = 0.1% is not applicable. The plots of $|\eta^*|(\gamma_0\omega)$ overlap at large strains with each other and with $\eta(\dot{\gamma})$, implying that the nonlinear response, observed after yielding, is quite similar and comparable. All mayos thus display the behavior $(\eta(\dot{\gamma}) = |\eta^*(\gamma_0\omega)|)$ anticipated by the extended Cox–Merz rule, also known as the Rutgers–Delaware rule. In such cases, the strain is large enough to significantly perturb the microstructure, as seen in Fig. 5 with strains of γ_0 = 30% and γ_0 = 40%.

In 1983, Bistany and Kokini[85] showed that a two-parameter modification of the Cox–Merz rule, $\eta^*(\omega) = C[\eta(\dot{\gamma})]^{\alpha}|_{\dot{\gamma}=\omega}$ with the exponent, α (ranging from 0.74 to 1.4) and a pre-factor, C (ranging from 0.160 to 9.52) captures the rate-dependent variation in apple butter, mustard, mayonnaise, and margarine. Berland and Launay suggested using α = 1 for wheat flour doughs[83] and this worked well for tapioca starch dispersions.[82] All empirical relationships are helpful if their range, domain and circumstances of validity are respected. However, the Rutgers–Delaware rule (aka the extended Cox–Merz rule) proposed by Doraiswamy *et al.*[75] is built on a stronger conceptual basis by accounting for a limiting recoverable strain that has a maximum value corresponding to the strain at which the transition from solid-like to liquid-like response (yielding) occurs. Recent studies by Shim *et al.*[106] offer a fundamental and valuable perspective using recovery rheology, which involves decomposing the strain into recoverable and unrecoverable parts. Shim *et al.*[106] find that the Rutgers–Delaware rule applies when the maximum imposed strain is high enough to yield the sample, where most of the strain is unrecoverable. Further exploration into microstructural recovery and recoverable elastic strain of mayonnaise will be detailed in a future study.

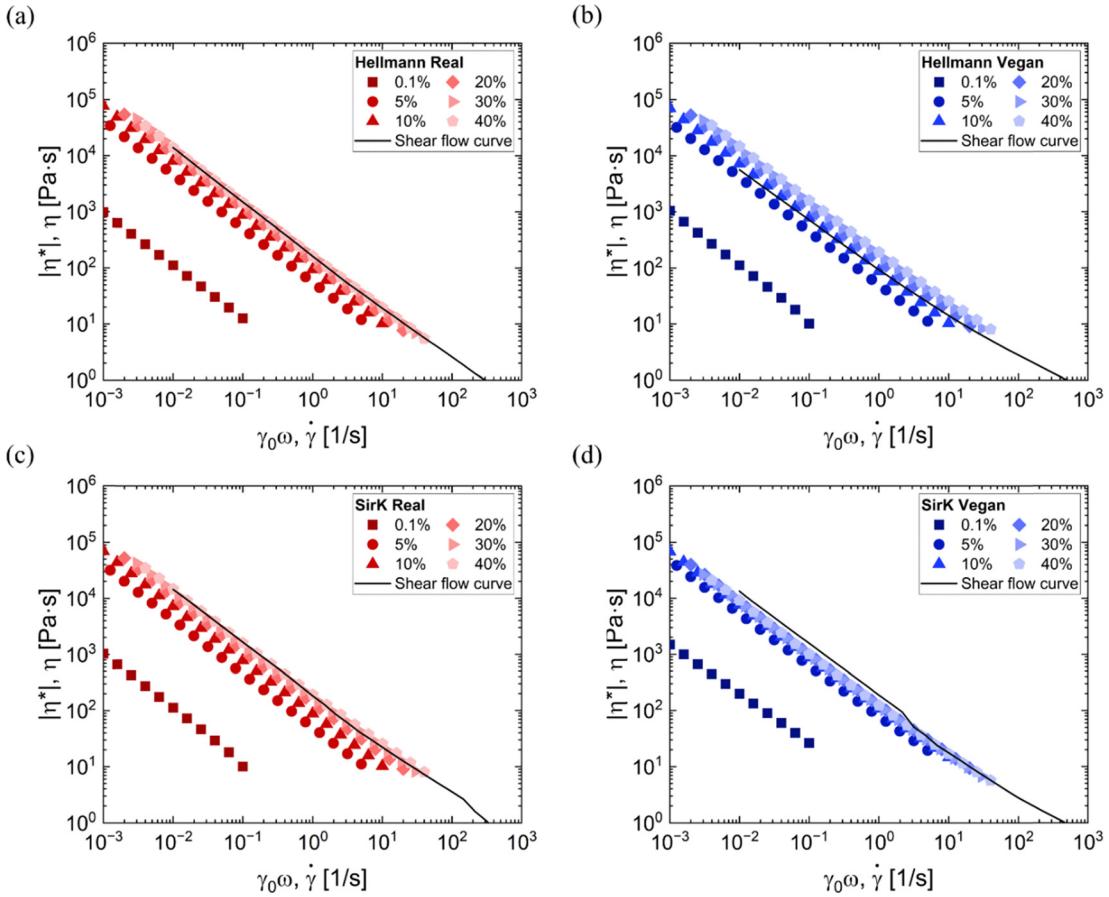

Fig. 5 Shear thinning behavior of real and vegan mayos and the Rutgers–Delaware rule. Magnitude of complex viscosity from frequency sweeps with indicated strain setting and shear rate dependent viscosity obtained using flow curves of Hellmann's (a) real mayonnaise and (b) vegan mayo and Sir Kensington's (c) real mayonnaise and (d) vegan mayo. Geometry used: roughened 25 mm parallel plates at 25 °C. Complex viscosity $|\eta^*|$ is plotted *versus* $\gamma_0\omega$ with filled symbols, and flow curve viscosity η is plotted against $\dot{\gamma}$ with solid black line.

The many avatars of yielding

Fig. 6 illustrates three manifestations of yield stress in the rate-dependent stress variation in a flow curve, strain-dependent storage and loss moduli at a fixed oscillation frequency, and images with an increasing length-dependent weight for real Hellmann's mayo in the top row (Fig. 6a–c) and vegan Hellmann's mayo samples in the second row (Fig. 6d–f). Fig. 6a and d show that the standard flow curves for AB and PB samples can be fitted to the Herschel–Bulkey (HB) model.[107] The HB model combines a power law equation that captures the flow behavior at high rates with a "zero shear" or low shear value, corresponding to the yield stress, σ_y as shown in eqn (1):

$$\sigma = \sigma_y + K\dot{\gamma}^n \quad (1)$$

Fig. 6b and e consider yielding as manifested in oscillatory shear and the determination of yield stresses. As discussed earlier in the context of Fig. 2, the elastic modulus displays strain softening above the critical strain, γ_c for all real and vegan mayos, and moduli show a shift from a solid-like $(G'(\gamma) > G''(\gamma))$ to a liquid-like $(G'(\gamma) < G''(\gamma))$ response above the crossover strain, γ_x. Either of the two strains can be used to identify the yielding point and determine an apparent yield stress; both values are listed in Table 3. In the first case, yielding is indicated by the drop-off of the storage modulus from the linear regime. Using the moduli G'_c and G'_x observed at γ_c and γ_x, respectively, provide the two yield stress estimates, determined with the equation shown below, where $G'_c \approx 0.9G'_0$:

$$\sigma_y = G'_c\gamma_c \text{ or } \sigma_y = G'_x\gamma_x \quad (2)$$

Fig. 6c and f show a montage of dispensing and pinching, outlining solid-like and liquid-like regimes. The images are snapshots from an earlier study,[4] in which we determined the extensional yield stress, σ_{ye}, using dripping into air with gravity-based rheometry protocols.[108–111] Experimentally, the mayo was dispensed at a very slow flow rate, resulting in a nearly solid-like cylinder being extruded. Once the mass of the extrudate divided by the local area exceeded the yield stress, locally the material yielded and then underwent rapid pinching, as seen in Fig. 6c and f. The mass of the drop was directly measured after pinch-off, and the yielding event was considered at the onset of pinching, $0.9R_0$, where R_0 is the radius of

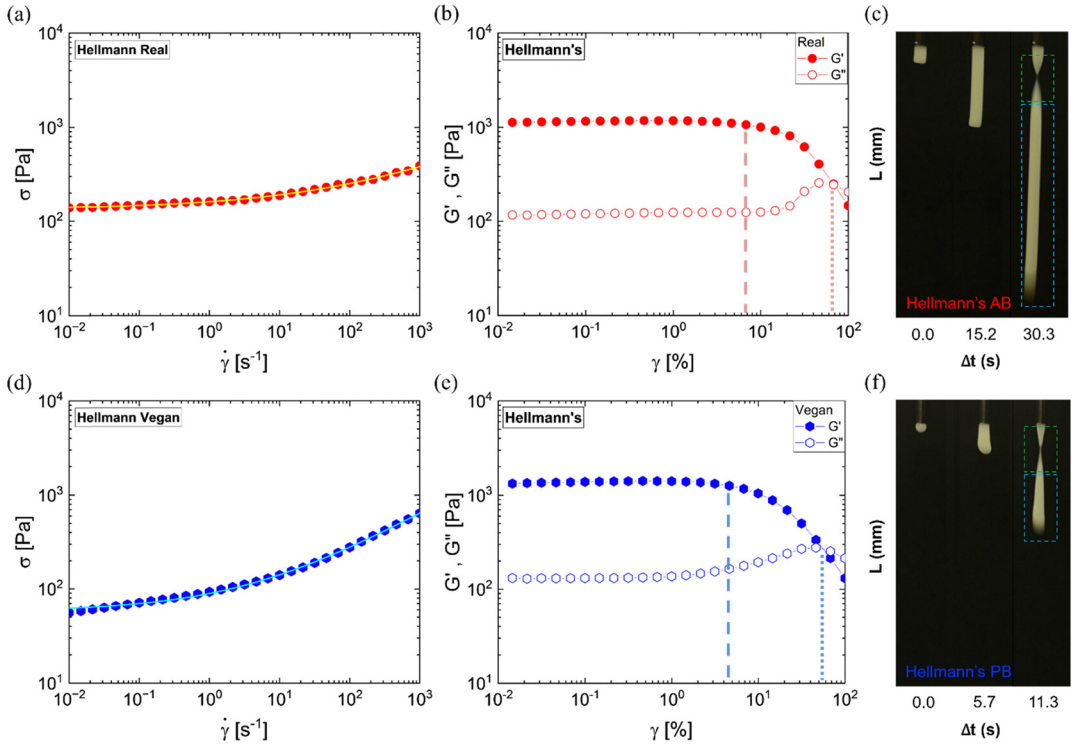

Fig. 6 Yielding in shear, oscillatory shear, and extension. (a) Flow curve of Hellmann's real mayonnaise with HB fit shown as a yellow line and (d) Hellmann's vegan mayo with HB fit shown as light blue line. Strain amplitude sweep of (b) Hellmann's real mayonnaise and (e) Hellmann's vegan mayo from oscillatory shear experiments. Yielding determined by drop-off from the LVE regime is indicated by the dashed line. Dotted lines indicate yielding determined by G', G'' crossover. Extensional yield stress is determined from the onset of pinching, $0.9R_0$, using edge-detection software in pinching videos for (c) Hellmann's real mayonnaise and (f) Hellmann's vegan mayo.

Table 3 LVE modulus and apparent yield stress calculated for real and vegan mayos

Sample	G_0' [Pa]	σ_y ($\dot{\gamma}$) [Pa]	γ_c [—]	σ_y (γ_c) [Pa]	γ_x [—]	σ_y (γ_x) [Pa]	$\sigma_{y,e}/\sqrt{3}$ [Pa]
Real: Hellmann's	1167	135	6.8	72	70.0	170	159
Real: Sir Kensington's	1077	151	14.6	133	73.9	174	142
Real: Kraft	853	161	10	74	68.9	123	123
Vegan: Hellmann's	1407	58	4.6	58	59.0	156	114
Vegan: Sir Kensington's	1707	89	1	15	55.8	109	98
Vegan: Chosen Foods	155	27	2.15	2.8	54.9	15	78
Vegan: Follow Your Heart	2387	161	2.15	46	37.5	121	152

the nozzle. Then, the extensional yield stress was determined using eqn (3), accounting for the weight of the droplet and the cross-sectional area of the flowing, pinching filament.

$$\sigma_{ye} = \frac{mg}{\pi(0.9R_0)^2} \quad (3)$$

The weight of the drop, the length or volume of the drop, and the timescale for pinch-off were higher for AB mayos, implying these tests visualize and illustrate differences that could manifest on dipping and dispensing.

Table 3 lists the values of yield stress, estimated using the following four distinct methods across varying experiments for all mayos: the shear flow curve (using the HB fit), strain sweep in oscillatory shear (using a choice of either critical strain or crossover strain, and the associated modulus), and dripping-into-air (DiA: relying on the interplay of yield stress and gravity for the onset of neck pinching, with capillarity playing a role before pinch-off). Yield stress, or the apparent yield stress, provides a pragmatic parameter for comparing materials and describing the stark change in viscosity or flow behavior that occurs with varying stress. However, the frequency chosen for oscillatory shear, the deformation history in dripping, the presence or absence of thixotropy for shear and extension, and the choice of protocols can all influence the absolute value of the apparent yield stress.[1,8,9,11,64,108,112–114] Regardless of the experimental method or the yielding criteria, vegan mayo samples showed lower yield stress than real mayonnaise samples.

In Table 3, the first column shows the elastic modulus magnitude from the LVE regime, observed before yielding, while the second column displays the yield stress. The apparent

yield stress for Hellmann's real mayonnaise (G'_c = 1063 Pa, γ_c = 6.79%) of σ_y = 72 Pa is larger than the corresponding value of σ_y = 58 Pa observed for the Hellmann's vegan mayo (yield point at G'_c = 1263 Pa, γ_c = 4.63%), calculated using eqn (1). Alternatively, the yield stress shown in the second-to-last column was determined from the crossover point between the elastic and viscous moduli or the transition from solid-like $G' > G''$ to liquid-like $G'' > G'$ behavior. The crossover point was determined by linear interpolation of the two neighboring data points of each modulus, followed by using the crossover modulus and crossover strain values in eqn (2). Table 3 also includes the values of extensional yield stress, σ_{ye}. To compare its value to yield stress manifested in shear rheometry, the last column entry is scaled by $\sqrt{3}$, as a von Mises yield criteron predicts $\sigma_{ye} = \beta\sigma_y$ with $\beta = \sqrt{3}$ though $\beta = \sqrt{3}$ to $\beta = 3\sqrt{3}$ are observed in experiments.[4,109,111,115] While shear rheology captures the response to shear flows involving velocity gradients perpendicular to the flow direction arising during pumping through tubes and orifices, or during spreading and dipping, extensional flows associated with streamwise velocity gradients that arise in dispensing, swallowing, and oral coating, making the extensional rheology response crucial for understanding oral processing, creaminess and cohesion.[19,28,116] Extensional rheology response is said to be more closely correlated with consumer-relevant performance in real-use scenarios such as squeezing or dolloping from a bottle, and spreading or spreadability.[8,10,19,20,41,42,77,109,110,116] Given the trends displayed by shear and extensional yield stress datasets, it appears plausible that the yield stress and the magnitude and the variation of the moduli can also indicate initial texture perception, the first-bite impression, firmness, and gel strength of soft materials like mayonnaise.[18,89] On similar lines, it can be said that the change in elastic and loss modulus as a function of strain or frequency imbibe insights into gel strength, yielding, microstructural changes, contributions to flow response, and heuristic and sensory properties.

At the high ϕ limit, for emulsions with similar interfacial, dispersed, and suspending fluid properties (all rheologically Newtonian), smaller drop sizes and narrower drop-size distributions are expected to yield higher yield stress, σ_y and elastic modulus.[35,37] However, σ_y asymptotically reaches a value set by capillary stress (ratio of surface tension to the drop size) at the highest ϕ or fat fraction, making emulsions with nearly monodisperse drops quite insensitive to volume fraction deep in the jammed-dense regime, $\phi > 70\%$.[35,37] Such explanations are inadequate for real formulations like mayos, as these theoretical and phenomenological arguments do not account for the non-Newtonian rheology of the interfacial and suspending fluids, and the physicochemical properties of the molecular, macromolecular, or particulate additives present in drops, thin films, and at interfaces, which affect emulsification, emulsion stability, and rheology.[4,35,37,92,117] Mayonnaise also traditionally contains mustard seed particles, and vegan mayos often contain additives like starch granules and polysaccharides. Among real mayos, the use of whole egg or addition of egg albumin provides for a more viscoelastic matrix (*e.g.* in Hellmann's real). In contrast, in vegan mayo, proptein–polysaccharide interactions can play a role.

The conformation- and interaction-dependent rheological properties of rheology modifiers such as cellulose gum and xanthan gum that are polyelectrolytes, show sensitivity to acid and electrolyte concentrations, and therefore are affected by the amount of lemon juice (or vinegar) and salt in recipes.[3,19,26,28,29,41,60] Recent studies show that modified starch granules and protein-based microgel particles can populate the oil–water interfaces in vegan mayos, suggesting that their stability and rheology can be mechanistically similar to those of Pickering emulsions.[46,94,118,119] Focused investigations are needed to characterize and elucidate the influence of drop size distribution, microstructural differences and ingredients like hydrocolloids and plant proteins on the various features of the rheological response of mayos and similar jammed, dense emulsions. The comparison of the Hellmann's real and vegan mayos shows that the shear thinning response in the flow curve and weak strain hardening (WSO) in the strain-amplitude sweep in oscillatory shear can be made similar despite a significant difference in fat content and protein types. Despite the fat content of $\phi > 70\%$, vegan mayos containing polysaccharides in the suspending liquid phase and possibly at the o/w interfaces show an absence of an overshoot or WSO response.

Implications of contrasting oscillatory shear properties

Rheology influences the sensory appreciation of mouthfeel and texture during eating, as well as the oral processing and bolus cohesiveness during swallowing.[5,7,18–20] Therefore, rheological investigation can enable formulators to distinguish between ingredient-dependent and processing-dependent differences and match desirable sensory attributes of products before they reach the consumer.[18,120–122] Schädle *et al.*[38] showed that rheological measurements of consistency and tribological measurements of "firmness" are strongly correlated in low-fat mayonnaise, whereas "spreadability" is associated with yield stress. Richardson *et al.*[68] argued that the sensory perception of thickness is correlated with the magnitude of complex viscosity, whereas stiffness is often correlated with the gel strength.[77] For completeness, the magnitude of complex modulus obtained as a function of frequency using SAOS and the magnitude of complex viscosity at effective shear rate (product of strain and frequency) are included in Fig. SF3 in the supplementary document. As thickness perception is often estimated by the viscosity measured at a shear rate, $\dot{\gamma}$ = 50 s^{-1}, the frequency-dependent response at matched deformation rate could be expected to correlate with thickness perception. However, this is only the first bite impression of texture during eating or consumption.[18] In reality, oral processing is complex and involves a broad and dynamic range of shear rates, often spanning from $\dot{\gamma} < 1$ s^{-1} (saliva mixing and coating) to $\dot{\gamma} > 10^3$ s^{-1} (mastication and swallowing) and a broad range of oscillatory strain and strain rates. The deformation rate continuously changes as the interfacial gap narrows during lubricated squeeze flow in the oral cavity, and the flow field exhibits both shear and extensional characteristics. Thus, real-life mouthfeel would be better captured across a range of shear rates,

referring to the viscosity profile within such a range to comprehensively assess the in-mouth performance of food products, with complementary deductions made using tribological and extensional rheology measurements and by accounting for the role played by dissolution, dilution and digestion brought about by the continuous addition of saliva.[116,123] Furthermore, mechanistic insights into how interfacial properties—such as interfacial tension, film elasticity, and adsorption kinetics—influence emulsion stability, drop deformation, and ultimately rheological and tribological responses would enhance and inform ingredient selection to optimize processing and sensory performance.

Though the variation in G' and G'' (and the flow curves) due to the choice of ingredients likely alters the consumer's overall experience and perception of "creaminess" and "thickness",[69,72,73,124] these sensory attributes only partially correlated with the rheological and tribological response.[18,68,70,71,125,126] Creaminess is a complex interaction between food and saliva in the mouth that results in the coalescence of dispersed oil droplets and a change in the suspending fluid fraction and properties, thereby altering the fluid and flow properties.[18,123,127] "Thickness", "stringiness", and "gloopiness" are heuristic perceptions of flow behavior, often illustrated and estimated using simple, handy or kitchen flow experiments like dripping from a ladle, dispensing from a bottle, stretching a liquid bridge between a thumb and index finger, between a dipped fry and mayo, or between a fruit and chocolate syrup; all include the influence of shear and extensional rheology and free surface flows. These consumer perceptions of flow behavior likely correlate with the strain-dependent and frequency-dependent changes in the oscillatory shear measures (G' and G''), as ultimately all connect to the role of dispersed macromolecules, drops, and particles, colloidal forces, and microstructural deformation. We infer that oscillatory shear enables characterization of three key features of flow behavior of mayo and other yield stress formulations – the apparent yield stress (from strain amplitude sweep), apparent shear thinning (from complex viscosity as a function of effective shear rate), and strain-dependent softening or stiffening (from G' and G'' at a fixed frequency). Yield stress, gel strength, rate or frequency dependent viscosity, and power law index, determined from oscillatory shear rheology provide pragmatic metrics for contrasting processability and sensory attributes.

Conclusions

We characterized the rheology and texture of animal-based and plant-based mayo emulsions *via* oscillatory shear measurements. The gel strength of animal-based mayonnaise was typically higher than that of vegan mayo, and the gel strength of vegan mayo varied significantly. A loss modulus strain overshoot was observed in the amplitude strain sweep of all real mayonnaises and some vegan mayo samples. The apparent yield stress was estimated for all mayos using four methods: the Herschel–Bulkley fit to the shear flow curve, a choice of either critical strain or crossover strain, and associated modulus from the strain sweep in oscillatory shear, and lastly, the volume of dispensed drop using dripping-into-air (DiA) experiments. Although the magnitude of yield stress varies with the calculation method, real mayos typically showed higher yield stress values than vegan mayos. All AB and PB mayos exhibited convergence between the viscosity *vs.* shear rate curves and variation in the magnitude of complex viscosity over a similar range of effective shear rate suggesting that the Rutgers–Delaware rule (or the extended Cox-Merz rule) is followed for these systems. The success of the Rutgers–Delaware rule implies that dynamic oscillatory shear tests can be used to gain an understanding of flow behavior relevant to the processing of flowing dense emulsions. The presence of apparent yield stress and gel-like behavior are characteristic of jammed-dense emulsions like real mayonnaise that contain polygonal oil drops within the network of thin liquid films and channels formed by the suspending aqueous phase. The influence of deformation-rate-dependent resistance to drainage or squeeze flows within thin films determines the rate-dependent viscosity. Smaller drop sizes and narrower drop-size distributions were measured for AB mayonnaises using non-invasive TD-NMR protocols. Our limited examination of drop sizes and fat content in vegan mayos shows larger sizes and lower overall oil fraction, in agreement with the literature. However, commercial vegan mayos can emulate the shear rheological response of AB mayos by using additives that influence interfacial and suspending fluid properties. Evaluating static (texture/consistency) and dynamic (mouthfeel) aspects through rheology and tribology can enable more targeted formulation strategies. In the future, integrating measures of shear and extensional flow can clarify how different deformation modes influence consumer-perceived creaminess and cohesiveness, particularly in spoonable and squeezable formats. Likewise, consistency, often assessed through the evaluation of viscosity and yielding behavior, can be used to contrast texture and perceived mouthfeel. A more suitable choice of hydrocolloids like starches and gums (or polysaccharides) requires a deeper appreciation of the role of surface-active ingredients that influence interfacial properties—such as interfacial tension, film elasticity, and adsorption behavior, and consequently modulate emulsion stability, flow behavior, and ultimately sensory appeal across plant-based and traditional formulations. We envision experimental protocols described in our two complementary studies on mayo rheology can be used for assessing the role of hydrocolloids and animal or plant proteins in determining the rheological and tribological outcomes.

Conflicts of interest

There are no conflicts to declare.

Data availability

Supplementary information is available. See DOI: https://doi.org/10.1039/d5sm00775e.

All the datasets and plots included in the attached contribution, "Rheological matchup of real and plant-based mayo: gel strength, strain overshoot, and yielding, plus the extended Cox–Merz rule," are available *via* request to the corresponding author.

Acknowledgements

We wish to acknowledge very insightful discussions with Michael Boehm (Mondelez), Christopher Zhang and Marjorie Welchoff (Ingredion), and Reza Foudazi (University of Oklahoma). We owe a debt of gratitude to Shamsheer Mahammad (Kraft Heinz) for very insightful comments on several aspects of measurements and analysis, and for providing us with drop size as well as compositional measurements. Discussions with many current and former members of the ODESlab are acknowledged, too, and NN wishes to thank the Department of Chemical Engineering for the support during the early stages of this research effort. Lastly, VS and NN ackowledge funding from Motif Foodworks Inc.

References

1 J. R. Stokes and W. J. Frith, *Soft Matter*, 2008, **4**, 1133–1140.
2 M. Langton, E. Jordansson, A. Altskär, C. Sørensen and A.-M. Hermansson, *Food Hydrocolloids*, 1999, **13**, 113–125.
3 L. Ma and G. V. Barbosa-Cánovas, *J. Food Eng.*, 1995, **25**, 409–425.
4 N. N. Nikolova, C. D. V. M. Narváez, L. Hassan, R. A. Nicholson, M. W. Boehm, S. K. Baier and V. Sharma, *Soft Matter*, 2023, **19**, 9413–9427.
5 M. A. Rao, *Rheology of Fluid and Semisolid Foods: Principles and Applications*, 2007, pp. 223–337.
6 D. J. McClements, *Food Emulsions: Principles, Practices, and Techniques*, CRC Press, 2015.
7 R. G. Larson, *The Structure and Rheology of Complex Fluids*, Oxford University Press, New York, 1999.
8 P. Coussot, *Rheol. Acta*, 2025, 1–27.
9 H. A. Barnes, *J. Non-Newtonian Fluid Mech.*, 1999, **81**, 133–178.
10 N. J. Balmforth, I. A. Frigaard and G. Ovarlez, *Annu. Rev. Fluid Mech.*, 2014, **46**, 121–146.
11 A. Z. Nelson, K. S. Schweizer, B. M. Rauzan, R. G. Nuzzo, J. Vermant and R. H. Ewoldt, *Curr. Opin. Solid State Mater. Sci.*, 2019, **23**, 100758.
12 H. McGee, *On Food and Cooking: the Science and Lore of the Kitchen*, Scribner, New York, Completely Revised and Updated edn, 2004.
13 M. Brenner, P. Sörensen and D. Weitz, *Science and Cooking: Physics meets Food, from Homemade to Haute Cuisine*, WW Norton & Company, New York, 2020.
14 M. W. Boehm, R. A. Nicholson and S. K. Baier, *Curr. Opin. Food Sci.*, 2022, 100982.
15 Y. He, S. K. Purdy, T. J. Tse, B. Tar'an, V. Meda, M. J. Reaney and R. Mustafa, *Foods*, 2021, **10**, 1978.
16 Z. Ma and J. I. Boye, *Food Bioprocess Technol.*, 2013, **6**, 648–670.
17 V. Raikos, H. Hayes and H. Ni, *Int. J. Food Sci. Technol.*, 2020, **55**, 1935–1942.
18 J. R. Stokes, M. W. Boehm and S. K. Baier, *Curr. Opin. Colloid Interface Sci.*, 2013, **18**, 349–359.
19 P. Fischer and E. J. Windhab, *Curr. Opin. Colloid Interface Sci.*, 2011, **16**, 36–40.
20 A. Ahuja, J. Lu and A. Potanin, *J. Texture Stud.*, 2019, **50**, 295–305.
21 E. C. Y. Li-Chan and H. O. Kim, *Egg Biosci. Biotechnol.*, 2008, **10**, 9780470181249.
22 X. Jing, Y. Cai, T. Liu, B. Chen, Q. Zhao, X. Deng and M. Zhao, *Food Chem.*, 2023, **403**, 134337.
23 V. Nikzade, M. M. Tehrani and M. Saadatmand-Tarzjan, *Food Hydrocolloids*, 2012, **28**, 344–352.
24 J. Yang and L. M. C. Sagis, *Curr. Opin. Colloid Interface Sci.*, 2021, **56**, 101499.
25 E. Armaforte, L. Hopper and G. Stevenson, *LWT–Food Sci. Technol.*, 2021, **136**, 110341.
26 E. Dickinson, *Food Hydrocolloids*, 2009, **23**, 1473–1482.
27 P. A. Williams and G. O. Phillips, *Handbook of Hydrocolloids*, Elsevier, 2021, pp. 3–26.
28 L. N. Jimenez, C. D. V. Martínez Narváez and V. Sharma, *Phys. Fluids*, 2020, **32**, 012113.
29 L. N. Jimenez, C. D. V. Martínez Narváez and V. Sharma, *Macromolecules*, 2022, **55**, 8117–8132.
30 L. Hassan, K. Al Zahabi, N. N. Nikolova, M. W. Boehm, S. K. Baier and V. Sharma, *Phys. Fluids*, 2025, **37**, 043112.
31 D. J. McClements and L. Grossmann, *Compr. Rev. Food Sci. Food Saf.*, 2021, **20**, 4049–4100.
32 P. Erni, E. J. Windhab and P. Fischer, *Macromol. Mater. Eng.*, 2011, **296**, 249–262.
33 P. Fischer and P. Erni, *Curr. Opin. Colloid Interface Sci.*, 2007, **12**, 196–205.
34 R. Foudazi, S. Qavi, I. Masalova and A. Y. Malkin, *Adv. Colloid Interface Sci.*, 2015, **220**, 78–91.
35 H. S. Kim and T. G. Mason, *Adv. Colloid Interface Sci.*, 2017, **247**, 397–412.
36 D. Langevin, *Emulsions, Microemulsions and Foams*, Springer, 2020.
37 R. B. Reboucas, N. N. Nikolova and V. Sharma, *Curr. Opin. Colloid Interface Sci.*, 2025, **77**, 101904.
38 C. N. Schädle, S. Bader-Mittermaier and S. Sanahuja, *Foods*, 2022, **11**, 806.
39 M. R. Serial, L. N. Arnaudov, S. Stoyanov, J. A. Dijksman, C. Terenzi and J. P. M. van Duynhoven, *Molecules*, 2022, **27**, 3070.
40 J. A. Goshawk, D. M. Binding, D. B. Kell and R. Goodacre, *J. Rheol.*, 1998, **42**, 1537–1553.
41 A. E. Blok, D. P. Bolhuis, L. N. Arnaudov, K. P. Velikov and M. Stieger, *Food Hydrocolloids*, 2023, **136**, 108242.
42 K. Maruyama, T. Sakashita, Y. Hagura and K. Suzuki, *Food Sci. Technol. Res.*, 2007, **13**, 1–6.
43 V. D. Kiosseoglou and P. Sherman, *J. Texture Stud.*, 1983, **14**, 397–417.
44 M. Taslikh, N. Mollakhalili-Meybodi, A. M. Alizadeh, M.-M. Mousavi, K. Nayebzadeh and A. M. Mortazavian, *J. Food Sci. Technol.*, 2022, **59**, 2108–2116.
45 R. C. F. de Menezes, Q. C. de Carvalho Gomes, B. S. de Almeida, M. F. R. de Matos and L. C. Pinto, *Int. J. Gastronomy Food Sci.*, 2022, **30**, 100599.

46 E. Taghavi, C. Andriani, N. Nordin, A. Z. R. Awang Seruji, N. Wan Rasdi and N. Abdul Hadi, *Int. J. Food Sci. Technol.*, 2024, **59**, 5651–5663.
47 A. Gemant, *Trans. Faraday Soc.*, 1935, **31**, 1582–1589.
48 D. C. Vadillo, C. E. Owens, A. Perego and G. H. McKinley, *Rheol. Acta*, 2025, 1–21.
49 K. Hyun, M. Wilhelm, C. O. Klein, K. S. Cho, J. G. Nam, K. H. Ahn, S. J. Lee, R. H. Ewoldt and G. H. McKinley, *Prog. Polym. Sci.*, 2011, **36**, 1697–1753.
50 H. S. Joyner, *Annu. Rev. Food Sci. Technol.*, 2021, **12**, 591–609.
51 A. N. M. Le, M. Y. Erturk, Y. H. Shim, S. A. Rogers and J. Kokini, *Food Res. Int.*, 2023, **174**, 113587.
52 M. Yoshida, D. Nakagawa, H. Hozumi, Y. Horikawa, S. Makino, H. Nakamura and T. Shikata, *Biomacromolecules*, 2024, **25**, 3420–3431.
53 D. E. Ngouémazong, F. F. Tengweh, I. Fraeye, T. Duvetter, R. Cardinaels, A. Van Loey, P. Moldenaers and M. Hendrickx, *Food Hydrocolloids*, 2012, **26**, 89–98.
54 I. Verlent, M. Hendrickx, P. Rovere, P. Moldenaers and A. V. Loey, *J. Food Sci.*, 2006, **71**, S243–S248.
55 O. C. Duvarci, G. Yazar and J. L. Kokini, *J. Food Eng.*, 2017, **208**, 77–88.
56 Q. Wen, A. Basu, J. P. Winer, A. Yodh and P. A. Janmey, *New J. Phys.*, 2007, **9**, 428.
57 C. Storm, J. J. Pastore, F. C. MacKintosh, T. C. Lubensky and P. A. Janmey, *Nature*, 2005, **435**, 191–194.
58 N. Lowithun, L. M. C. Sagis and N. Lumdubwong, *Foods*, 2024, **13**, 1864.
59 K. Hyun, S. H. Kim, K. H. Ahn and S. J. Lee, *J. Non-Newtonian Fluid Mech.*, 2002, **107**, 51–65.
60 J. E. Martín-Alfonso, A. A. Cuadri, M. Berta and M. Stading, *Carbohydr. Polym.*, 2018, **181**, 63–70.
61 L. Martinetti, O. Carey-De La Torre, K. S. Schweizer and R. H. Ewoldt, *Macromolecules*, 2018, **51**, 8772–8789.
62 G. Tabilo-Munizaga and G. V. Barbosa-Cánovas, *J. Food Eng.*, 2005, **67**, 147–156.
63 A. Sun and S. Gunasekaran, *Int. J. Food Prop.*, 2009, **12**, 70–101.
64 J. J. Griebler and S. A. Rogers, *Phys. Fluids*, 2022, **34**(2), 023107.
65 M. Dinkgreve, J. Paredes, M. M. Denn and D. Bonn, *J. Non-Newtonian Fluid Mech.*, 2016, **238**, 233–241.
66 D. Bonn, M. M. Denn, L. Berthier, T. Divoux and S. Manneville, *Rev. Mod. Phys.*, 2017, **89**, 035005.
67 H. S. Melito, C. R. Daubert and E. A. Foegeding, *J. Food Process Eng.*, 2013, **36**, 521–534.
68 R. K. Richardson, E. R. Morris, S. B. Ross-Murphy, L. J. Taylor and I. C. M. Dea, *Food Hydrocolloids*, 1989, **3**, 175–191.
69 E. Dickinson, *Food Hydrocolloids*, 2018, **77**, 372–385.
70 Y. Pascua, H. Koç and E. A. Foegeding, *Curr. Opin. Colloid Interface Sci.*, 2013, **18**, 324–333.
71 R. Upadhyay, T. Aktar and J. Chen, *J. Texture Stud.*, 2020, **51**, 375–388.
72 H. Weenen, R. H. Jellema and R. A. De Wijk, *Food Quality Pref.*, 2005, **16**, 163–170.
73 H. Weenen, L. J. Van Gemert, J. M. Van Doorn, G. B. Dijksterhuis and R. A. De Wijk, *J. Texture Stud.*, 2003, **34**, 159–179.
74 W. P. Cox and E. H. Merz, *J. Polym. Sci.*, 1958, **28**, 619–622.
75 D. Doraiswamy, A. N. Mujumdar, I. Tsao, A. N. Beris, S. C. Danforth and A. B. Metzner, *J. Rheol.*, 1991, **35**, 647–685.
76 V. Sharma and G. H. McKinley, *Rheol. Acta*, 2012, **51**, 487–495.
77 S. Gunasekaran and M. M. Ak, *Trends Food Sci. Technol.*, 2000, **11**, 115–127.
78 R. D. McCurdy, H. D. Goff, D. W. Stanley and A. P. Stone, *Food Hydrocolloids*, 1994, **8**, 609–623.
79 E. K. Chamberlain and M. A. Rao, *Carbohydr. Polym.*, 1999, **40**, 251–260.
80 M. A. Rao and H. J. Cooley, *J. Texture Stud.*, 1992, **23**, 415–425.
81 M. A. Rao, P. E. Okechukwu, P. M. S. Da Silva and J. C. Oliveira, *Carbohydr. Polym.*, 1997, **33**, 273–283.
82 M. A. Rao and J. Tattiyakul, *Carbohydr. Polym.*, 1999, **38**, 123–132.
83 S. Berland and B. Launay, *Rheol. Acta*, 1995, **34**, 622–625.
84 C. Yu and S. Gunasekaran, *Appl. Rheol.*, 2001, **11**, 134–140.
85 K. L. Bistany and J. L. Kokini, *J. Rheol.*, 1983, **27**, 605–620.
86 I. M. Krieger, *J. Rheol.*, 1992, **36**, 215–217.
87 T. G. Mason, M.-D. Lacasse, G. S. Grest, D. Levine, J. Bibette and D. A. Weitz, *Phys. Rev. E:Stat. Phys., Plasmas, Fluids, Relat. Interdiscip. Top.*, 1997, **56**, 3150.
88 S. Marze, R. M. Guillermic and A. Saint-Jalmes, *Soft Matter*, 2009, **5**, 1937–1946.
89 M. E. J. Terpstra, A. M. Janssen, J. F. Prinz, R. A. De Wijk, H. Weenen and E. Van Der Linden, *J. Texture Stud.*, 2005, **36**, 213–233.
90 C. Gallegos, M. Berjano and L. Choplin, *J. Rheol.*, 1992, **36**, 465–478.
91 J. Muñtoz and P. Sherman, *J. Texture Stud.*, 1990, **21**, 411–426.
92 G. Katsaros, M. Tsoukala, M. Giannoglou and P. Taoukis, *Heliyon*, 2020, **6**(12), e05788.
93 C. Chang, J. Li, X. Li, C. Wang, B. Zhou, Y. Su and Y. Yang, *LWT–Food Sci. Technol.*, 2017, **82**, 8–14.
94 P. Chivero, S. Gohtani, H. Yoshii and A. Nakamura, *LWT–Food Sci. Technol.*, 2016, **69**, 59–66.
95 I. Ozcan, E. Ozyigit, S. Erkoc, S. Tavman and S. Kumcuoglu, *J. Food Eng.*, 2023, **344**, 111388.
96 A. Jabermoradi, S. Foroutanparsa, I. K. Voets, J. Janssen, J. P. van Duynhoven and J. Hohlbein, *Food Hydrocolloids*, 2025, 111490.
97 G. J. W. Goudappel, J. P. M. Van Duynhoven and M. M. W. Mooren, *J. Colloid Interface Sci.*, 2001, **239**, 535–542.
98 G. Colafemmina, H. Mateos and G. Palazzo, *Curr. Opin. Colloid Interface Sci.*, 2020, **48**, 109–120.
99 F. M. V. Pereira, A. P. Rebellato, J. A. L. Pallone and L. A. Colnago, *Food Control*, 2015, **48**, 62–66.
100 E. Kirtil, S. Cikrikci, M. J. McCarthy and M. H. Oztop, *Curr. Opin. Food Sci.*, 2017, **17**, 9–15.
101 H. M. Princen, *J. Colloid Interface Sci.*, 1983, **91**, 160–175.
102 H. M. Princen, *J. Colloid Interface Sci.*, 1985, **105**, 150–171.
103 H. M. Princen and A. D. Kiss, *J. Colloid Interface Sci.*, 1986, **112**, 427–437.

104 H. M. Princen and A. D. Kiss, *J. Colloid Interface Sci.*, 1989, **128**, 176–187.
105 F. Schott, B. Dollet, S. Santucci, C. M. Schlepütz, C. Claudet, S. Gstöhl, C. Raufaste and R. Mokso, *Nat. Commun.*, 2025, **16**, 9210.
106 Y. H. Shim, J. J. Griebler and S. A. Rogers, *J. Rheol.*, 2024, **68**, 381–396.
107 W. H. Herschel and R. Bulkley, *Kolloid-Z.*, 1926, **39**, 291–300.
108 P. Coussot and F. Gaulard, *Phys. Rev. E:Stat., Nonlinear, Soft Matter Phys.*, 2005, **72**, 031409.
109 N. J. Balmforth, N. Dubash and A. C. Slim, *J. Non-Newtonian Fluid Mech.*, 2010, **165**, 1147–1160.
110 A. Geffrault, H. Bessaies-Bey, N. Roussel and P. Coussot, *J. Rheol.*, 2021, **65**, 887–901.
111 A. Geffrault, H. Bessaies-Bey, N. Roussel and P. Coussot, *J. Rheol.*, 2023, **67**, 305–314.
112 R. Miriyala, A. P. Deshpande and P. Ravindran, *J. Food Eng.*, 2025, **397**, 112573.
113 T. Bhattacharyya, A. R. Jacob, G. Petekidis and Y. M. Joshi, *J. Rheol.*, 2023, **67**, 461–477.
114 P. R. de Souza Mendes and R. L. Thompson, *Rheol. Acta*, 2013, **52**, 673–694.
115 K. Niedzwiedz, O. Arnolds, N. Willenbacher and R. Brummer, *Appl. Rheol.*, 2009, **19**, 41969.
116 K. Al Zahabi, L. Hassan, R. Maldonado, M. W. Boehm, S. K. Baier and V. Sharma, *Soft Matter*, 2024, **20**, 2547–2561.
117 P. L. Fuhrmann, S. Breunig, G. Sala, L. Sagis, M. Stieger and E. Scholten, *J. Colloid Interface Sci.*, 2022, **607**, 389–400.
118 A. Akcicek, S. Karasu, F. Bozkurt and S. Kayacan, *ACS Omega*, 2022, **7**, 26316–26327.
119 S. Tcholakova, N. D. Denkov and A. Lips, *Phys. Chem. Chem. Phys.*, 2008, **10**, 1608–1627.
120 P. Sherman, *J. Food Sci.*, 1969, **34**, 458–462.
121 C. Wilkinson, G. B. Dijksterhuis and M. Minekus, *Trends Food Sci. Technol.*, 2000, **11**, 442–450.
122 J. Chen and J. R. Stokes, *Trends Food Sci. Technol.*, 2012, **25**, 4–12.
123 A. Sarkar, S. Soltanahmadi, J. Chen and J. R. Stokes, *Food Hydrocolloids*, 2021, **117**, 106635.
124 M. Akhtar, B. S. Murray and E. Dickinson, *Food Hydrocolloids*, 2006, **20**, 839–847.
125 T. L. Ditschun, E. Riddell, W. Qin, K. Graves, O. Jegede, N. Sharafbafi, T. Pendergast, D. Chidichimo and S. F. Wilson, *Compr. Rev. Food Sci. Food Saf.*, 2025, **24**, e70126.
126 J. Chen, *Food Hydrocolloids*, 2009, **23**, 1–25.
127 D. M. Dresselhuis, E. H. A. De Hoog, M. A. C. Stuart, M. H. Vingerhoeds and G. A. Van Aken, *Food Hydrocolloids*, 2008, **22**, 1170–1183.